ORIGINAL RESEARCH

miR-146a-5p mitigates ethanol-induced neuroinflammation by targeting Btg2-dependent microglial activation

Bo Cheng[1,*], Yan Wang[1], Ping Huang[2], Zikuo Dong[3], Junya Zhou[1], Guoqing Kang[3], Chengzhu Wang[3], Zhenkun Yan[1]

1. Department of Substance Dependence, The Fifth People's Hospital of Kaifeng, Kaifeng 475000, Henan, China.
2. Department of Psychiatry I, The Fifth People's Hospital of Kaifeng, Kaifeng 475000, Henan, China.
3. Director of The Hospital, The Fifth People's Hospital of Kaifeng, Kaifeng 475000, Henan, China.

*** Corresponding Author: Bo Cheng** E-mail: chengbo_edu@outlook.com

Abstract

Background

Chronic alcohol exposure leads to progressive neurodegeneration, primarily driven by sustained neuroinflammation and microglial activation. While microRNAs are key regulators of neuroimmune responses, the specific role of miR-146a-5p and its downstream targets in ethyl alcohol (EtOH)-induced neuroinflammatory injury remain poorly understood.

Methods

A chronic EtOH exposure model was established in C57BL/6 mice and BV-2 microglial cells. Neuroinflammatory damage was assessed using behavioral tests (Morris water maze), apoptosis assays, cytokine quantification, and immunostaining. The regulatory relationship between miR-146a-5p and its target gene Btg2 was investigated using luciferase reporter and RNA pull-down assays, combined with gain-of-function approaches.

Results

EtOH exposure significantly downregulated miR-146a-5p expression in both mouse hippocampal tissue and BV-2 cells. Overexpression of miR-146a-5p in vivo improved spatial learning and memory, reduced neuronal apoptosis, and attenuated microglial activation and pro-inflammatory cytokine (IL-1β, IL-6, TNF-α) production. Mechanistically, Btg2 was identified as a direct target of miR-146a-5p. EtOH-induced Btg2 upregulation was reversed by miR-146a-5p overexpression in vitro. Importantly, restoring Btg2 expression abolished the anti-inflammatory and anti-apoptotic effects of miR-146a-5p in EtOH-treated BV-2 cells.

Conclusion

This study identifies the miR-146a-5p/Btg2 axis as a critical regulator of EtOH-induced microglial activation and neuroinflammation. Targeting this pathway may offer a promising therapeutic strategy for alcohol-related neurodegeneration.

Keywords: alcohol, neuroinflammation, microglial activation, miR-146a-5p, Btg2

Introduction

Regional surveys indicate that the drinking rate among adults in China exceeds 59.0%. Notably, the rate is particularly high (68.0% to 70.3%) among individuals aged 30 to 50 years[1]. While acute alcoholism and addiction have garnered significant societal attention, with established institutions, regulations, and treatments, chronic alcoholism resulting from long-term consumption is often overlooked. This oversight is due to its prolonged incubation period and subtle symptomatology[2]. It has been reported that ethyl alcohol (EtOH) and its metabolites can directly act on the nervous system, and long-term stimulation will cause oxidative stress reaction leading to neurological damage, which is manifested as significant changes in electroencephalogram, memory impairment, inattention, and motor incoordination[3]. What's more, the structure of brain neurons is destroyed, leading to degenerative changes in the nervous system[4]. Because the change is irreversible, once clinical symptoms appear, it indicates that the nervous system has been permanently damaged[5]. However, the current clinical lack of relevant prevention and treatment methods, patients themselves are not strong, easy to miss the best treatment opportunities[6]. Therefore, there is an urgent need for treatment of chronic alcoholism to control the disease process and prevent degenerative changes in the nervous system.

Neuroinflammation is believed to have a critical role in alcohol-linked neurodegeneration, with microglia activation being central to the inflammatory response[7]. As the brain's primary innate immune cells, microglia maintain neural tissue homeostasis. They continuously survey the CNS parenchyma by extending and retracting their projections to detect damage or infection. Furthermore, they play a crucial role in ensuring proper synaptic function[8]. When the central nervous system sustains an injury or becomes infected, microglia are activated. They release a variety of inflammatory factors and adjust their phagocytic activity in order to combat the infection and promote nerve repair[9]. However, in many neuropsychiatric disorders, microglial immune function becomes dysregulated. This impairment leads to excessive production of inflammatory mediators and heightened phagocytic activity, ultimately exacerbating neuronal damage[10].

Recently, studies on the correlation between microRNAs (miRNAs) and neuroinflammation induced by chronic EtOH

https://dx.doi.org/10.4314/mmj.v38i2.12

exposure have attracted more and more attention[11]. MiRNAs are small noncoding RNAs that have 20-25 nucleotides in length[12]. About 2,200 miRNAs are reported to exist in mammalian genomes, and about one-third of the human genome can be modulated by miRNAs[13]. The miRNAs regulate gene expression post-transcriptionally[14], primarily by binding to the 3'-untranslated region (3'UTR) of target mRNAs[15]. This binding typically leads to mRNA degradation or translational repression, thereby modulating various physiological and pathological processes[16]. Over the past few years, research on miRNA has advanced rapidly, revealing its significant role in multifarious biological processes, containing metabolism, cell proliferation, apoptosis, as well as neuronal cell fate. Furthermore, miRNA takes part in the pathogenesis of neurodegenerative diseases[17]. Notably, miR-146a-5p has been documented to have a function in nervous system disorders. For example, it protects retinal ganglion cells by reducing neuroinflammation in experimental glaucoma[18] and alleviates chronic neuropathic pain by suppressing TRAF6 signaling[19]. Nevertheless, the specific function and molecular mechanism of miR-146a-5p in alcohol-induced neurotoxicity remain poorly understood.

In this research, our objective was to investigate miR-146a-5p's function and underlying mechanism in alcohol-induced nerve injury. We built a chronic alcohol exposure model using mice and BV-2 cells, and assessed miR-146a-5p's influences on neuroinflammation and microglial activation. Additionally, we explored the underlying molecular mechanism of miR-146a-5p in vitro. Furthermore, our findings imply miR-146a-5p has potential as a hopeful biomarker for alcohol-induced nerve injury.

Material and Methods

Animals

Male C57BL/6 mice (6-8 weeks old, weighing 18-22 g) were obtained from Aniphe BioLab (Nanjing, China). The mice were housed under controlled environmental conditions (22-25°C, 45-55% humidity) with a 12-hour light/dark cycle. Food and water were provided ad libitum. All experimental procedures were approved by the Experimental Animal Care and Use Committee of our hospital.

Construction of chronic alcohol exposure model

A chronic alcohol exposure model was established as previously described (20). Mice were randomly divided into four groups (n=6 per group): control group, model group, model+agomir NC group, and model+miR-146a-5p agomir group. Mice in the model group received 25% EtOH (w/v) via intragastric administration once daily at 9:00 AM for 28 consecutive days at a dose of 5 g/kg body weight/day. Both agomir NC and miR-146a-5p agomir were purchased from GenePharm (Shanghai, China). To deliver the agomirs to the brain, a stereotactic catheter was surgically implanted into the mice as detailed previously (21). A total of 5 μL of saline containing 20 nmol/L of either miR-146a-5p agomir or agomir NC was injected via the catheter daily for seven consecutive days. Stereotaxic coordinates for catheter implantation into the lateral ventricle were: anteroposterior (AP) = -2.0 mm from bregma, mediolateral (ML) = ±1.5 mm, dorsoventral (DV) = -2.0 mm from the dura mater. To validate the accuracy of the delivery site, an additional cohort of three mice (not included in the experimental groups) received an injection of 5 μL of 1% Evans Blue dye through the same catheter system. Thirty minutes after injection, mice were euthanized, and their brains were sectioned for histological examination. Only animals with clear Evans Blue staining within the ventricular system were considered to have correctly placed cannulas. Mice with misplaced cannulas (dye diffusion outside the ventricular area) were excluded from the study. All experimental mice in the four groups were confirmed to have correct cannula placement by post-mortem examination. The first injection was administered 2 hours after the final EtOH dose.

Morris water maze test

The water maze was a circular pool (160 cm in diameter, 60 cm in height) filled with water to a depth of 30 cm. The interior wall of the pool and the escape platform were painted black. The pool was divided into four equal quadrants designated north, south, east, and west. Geometric shapes were attached to the wall above each quadrant to serve as visual cues. A circular escape platform (10 cm in diameter) was submerged 2 cm below the water surface in the center of the southeast quadrant. The water temperature was maintained at 19-22°C, and the room was illuminated with indirect lighting.

Orientation navigation experiment

The training experiment was conducted over 5 consecutive days, preceded by a 2-day adaptation period during which mice were placed in the maze four times daily. In each training trial, mice were placed into one quadrant of the maze and allowed 120 seconds to locate the hidden platform. Consecutive trials were separated by a 60-second interval. If a mouse failed to find the platform within the allotted time, it was gently guided to the platform and allowed to remain there for 30 seconds. The progressive decrease in escape latency (the time taken to find the hidden platform) over the training days indicated successful acquisition of the spatial learning task.

Space exploration experiment

Twenty-four hours after the final training session, the platform was removed from the maze. Mice were placed into the pool from the northwest quadrant and allowed to swim freely for 120 seconds. Spatial memory was assessed by measuring the time spent in the target quadrant (where the platform had been located) and the number of entries into this quadrant. After each test, the mice were carefully removed from the maze, dried, and returned to their home cages with free access to food and water.

Hematoxylin and Eosin (H&E) staining

Mice were euthanized and transcardially perfused with 500 mL of 4% paraformaldehyde (Sigma-Aldrich, USA) at 4°C for 2 hours. The hippocampus was then carefully dissected at 4°C and post-fixed in the same fixative for 12 hours at 4°C in the dark. Subsequently, the tissues were embedded in paraffin and sectioned at a thickness of 4 μm. The hippocampal sections were stained with hematoxylin and eosin (H&E) to assess neuronal morphology. Briefly, sections were incubated overnight at 60°C, dewaxed, rehydrated through a graded EtOH series, and stained with hematoxylin and eosin (Sigma-Aldrich, USA).

TUNEL staining

Hippocampal tissues were collected for TUNEL staining. Sections were baked at 60°C, dewaxed in xylene, and rehydrated through a graded EtOH series. Next, the sections were incubated with proteinase K at 25°C, followed by treatment with the TUNEL reaction mixture (Beyotime,

https://dx.doi.org/10.4314/mmj.v38i2.12

Table 1 Primer sequences of genes

Gene	Forward (5'-3')	Reverse (5'-3')
miR-146a-5p	CCTGAGAAGTGAATTCCATGGG	TGGTGTCGTGGAGTCG
Btg2	CCCCCCGGTGGCTGCCTCCTATG	GGGTCGGGTGGCTCCTATCTA
U6	CTCGCTTCGGCAGCACA	AACGCTTCACGAATTTGCGT
GAPDH	TGGCCTTCCGTGTTCCTAC	GAGTTGCTGTTGAAGTCGCA

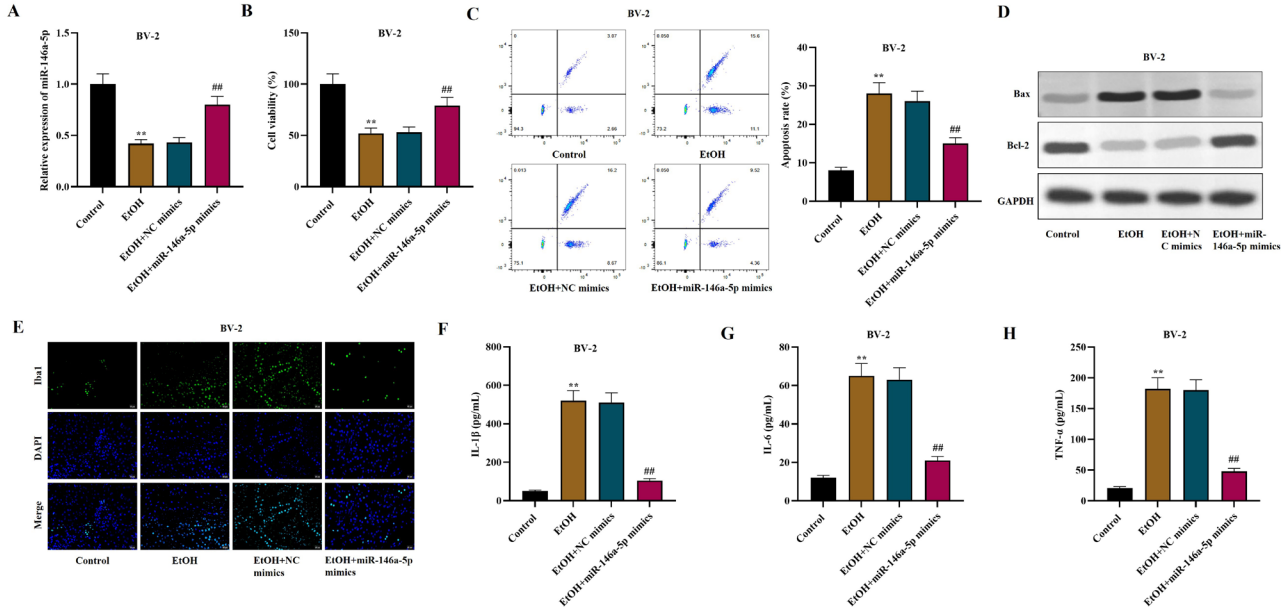

Figure 1 Overexpressed miR-146a-5p attenuated neuronal apoptosis, inflammation and microglial activation in EtOH-treated BV-2 cells. (A) RT-qPCR analysis of miR-146a-5p expression in BV-2 cells (Control, EtOH, EtOH+NC mimics and EtOH+miR-146a-5p mimics) (n=3 independent experiments). (B) CCK-8 assay of the viability in BV-2 cells (Control, EtOH, EtOH+NC mimics and EtOH+miR-146a-5p mimics) (n=6 technical replicates per experiment, 3 independent experiments). (C) Flow cytometry analysis of apoptosis rate in BV-2 cells (Control, EtOH, EtOH+NC mimics and EtOH+miR-146a-5p mimics) (n=3 independent experiments). (D) Western blot analysis of Bax and Bcl-2 protein levels in BV-2 cells (Control, EtOH, EtOH+NC mimics and EtOH+miR-146a-5p mimics). GAPDH served as loading control (representative of 3 independent experiments) (representative of 3 independent experiments). (E) Immunofluorescent staining of Iba-1 protein in BV-2 cells (Control, EtOH, EtOH+NC mimics and EtOH+miR-146a-5p mimics). Scale bar: 50 μm (images are representative of 3 independent experiments). (F-H) ELISA of pro-inflammatory cytokines (IL-1β, IL-6 and TNF-α) in BV-2 cells (Control, EtOH, EtOH+NC mimics and EtOH+miR-146a-5p mimics) (n=3 independent experiments). All quantitative data are presented as mean ± SD from three independent experiments. **P < 0.01 versus Control group; ##P < 0.01 versus EtOH group.

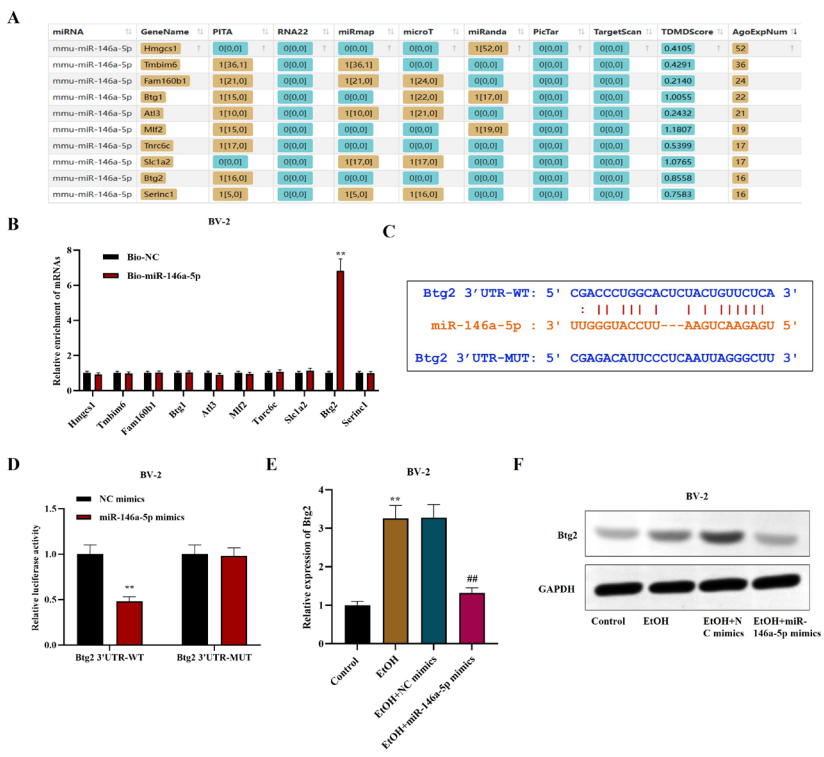

Figure 2 MiR-146a-5p targeted Btg2 in BV-2 cells. (A) The top 10 mRNAs of miR-146a-5p from starBase website. (B) RNA pull-down assay examined the binding between 10 mRNAs and miR-146a-5p in BV-2 cells (n=3 independent experiments). (C) Binding sequences between Btg2 3'UTR and miR-146a-5p. (D) Luciferase reporter assay measured the relative luciferase activity of Btg2 3'UTR-WT/MUT in BV-2 cells after miR-146a-5p mimics transfection (n=4 independent experiments). (E-F) RT-qPCR and western blot analyses of Btg2 expression in BV-2 cells (Control, EtOH, EtOH+NC mimics and EtOH+miR-146a-5p mimics) (n=3 independent experiments for qPCR; blot representative of 3 experiments). Data are presented as mean ± SD from the indicated number of independent experiments. **P < 0.01 versus Bio-NC, NC mimics, or Control group; ##P < 0.01 versus EtOH group.

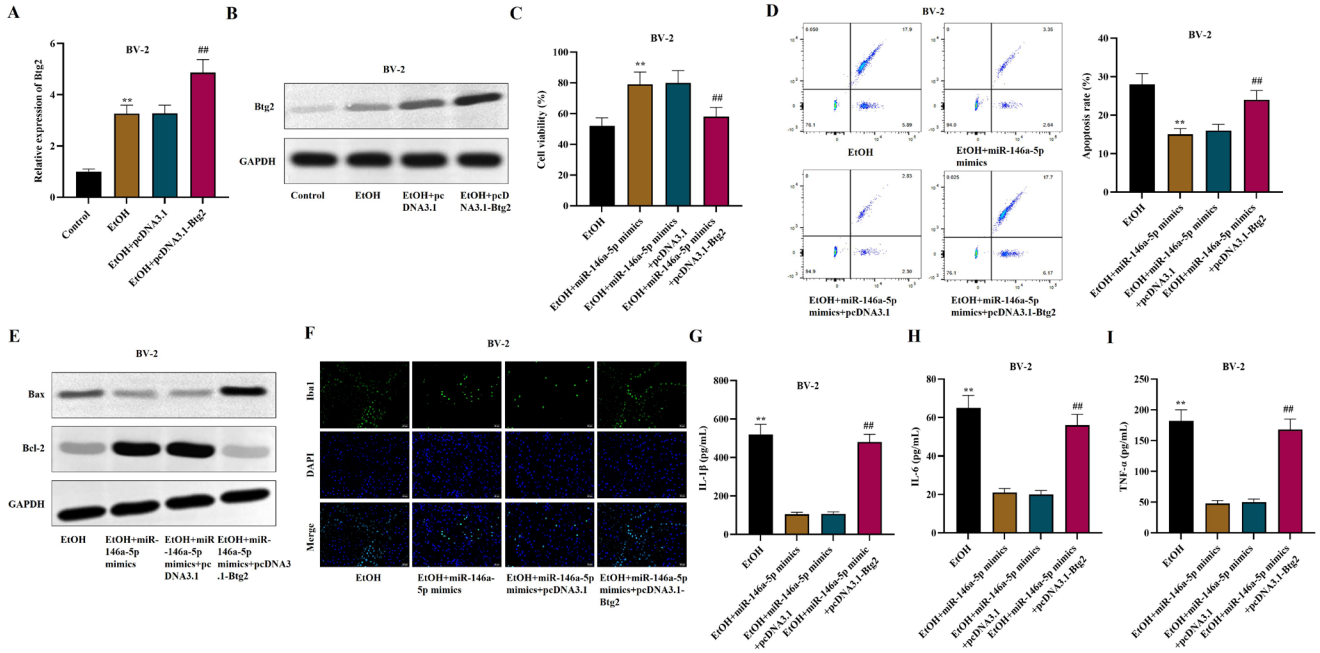

Figure 3 MiR-146a-5p attenuated neuronal apoptosis, inflammation and microglial activation in EtOH-treated BV-2 cells via targeting Btg2. (A-B) Validation of Btg2 overexpression. (A) RT-qPCR and (B) Western blot analysis of Btg2 expression in BV-2 cells treated as follows: Control (untreated), EtOH (200 mM ethyl alcohol), EtOH+pcDNA3.1 (empty vector control), EtOH+pcDNA3.1-Btg2 (Btg2-overexpression vector) (n=3 independent experiments). (C) Cell viability assessed by CCK-8 assay in BV-2 cells under four conditions: EtOH alone, EtOH+miR-146a-5p mimics, EtOH+miR-146a-5p mimics+pcDNA3.1, EtOH+miR-146a-5p mimics+pcDNA3.1-Btg2 (n=3 independent experiments). (D) Apoptosis rate measured by flow cytometry (Annexin V/PI staining) in the same four treatment groups as in (C) (n=3 independent experiments). (E) Western blot analysis of pro-apoptotic Bax and anti-apoptotic Bcl-2 protein levels under the four treatment conditions (representative of 3 independent experiments). (F) Representative immunofluorescence images showing Iba-1 expression (green, microglial marker) and DAPI (blue, nuclei) in the four treatment groups (representative of 3 experiments). Scale bar: 50 μm. (G-I) ELISA measurement of pro-inflammatory cytokine levels: (G) IL-1β, (H) IL-6, and (I) TNF-α in the culture supernatant of BV-2 cells under the four treatment conditions (n=3 independent experiments). Data are presented as mean ± SD of three independent experiments. **P < 0.01 versus Control and EtOH groups; ##P < 0.01 versus EtOH and EtOH+miR-146a-5p mimics groups.

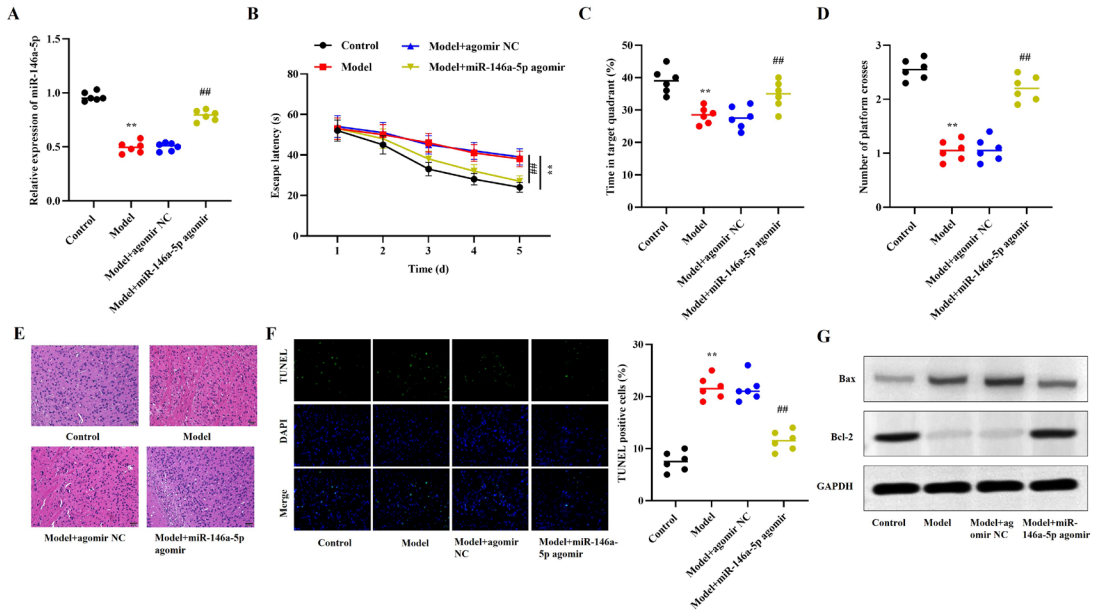

Figure 4 Overexpressed miR-146a-5p had a protective effect on alcohol-induced nerve damage in vivo. (A) RT-qPCR analysis of miR-146a-5p expression in hippocampal tissues from the four experimental groups (n=6 mice per group): Control (saline), Model (chronic alcohol exposure), Model+agomir NC (negative control agomir), Model+miR-146a-5p agomir. (B) Morris water maze performance: Escape latency (time to find the hidden platform) across 5 consecutive training days for each group (n=6). (C-D) Spatial memory probe test conducted 24 h after the last training session. (C) Time spent in the target quadrant (formerly containing the platform) and (D) number of platform crossings during a 120-s trial (n=6). (E) Representative H&E staining of hippocampal CA1 region sections showing neuronal morphology and structural integrity across the four groups (representative images from n=6 mice per group). Scale bar: 50 μm. (F) TUNEL staining (brown) detecting apoptotic cells in hippocampal sections. Nuclei are counterstained with hematoxylin (blue) (representative images from n=6 mice per group). Scale bar: 100 μm. (G) Western blot analysis of Bax and Bcl-2 protein expression in hippocampal lysates from the four experimental groups. GAPDH served as loading control (n=4 mice per group for quantification; blot shows representative samples). Data in bar graphs are presented as mean ± SD. **P < 0.01 versus Control group; ##P < 0.01 versus Model group.

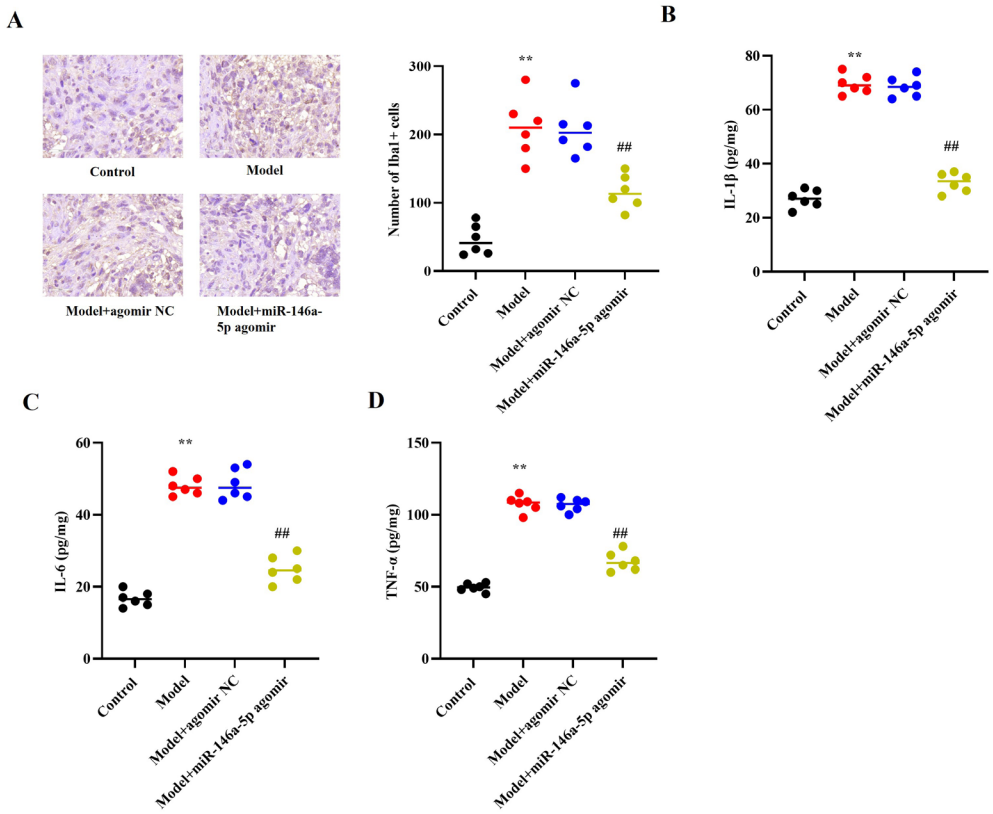

Figure 5 Overexpressed miR-146a-5p had a protective effect on alcohol-induced neuroinflammation and microglial activation in vivo. (A) Representative immunohistochemical staining for Iba1 (brown, microglial marker) in hippocampal sections from the four experimental groups (n=6 mice per group): Control, Model, Model+agomir NC, and Model+miR-146a-5p agomir. Nuclei are counterstained with hematoxylin (blue). Scale bar: 100 μm. (B-D) ELISA quantification of pro-inflammatory cytokines in hippocampal tissue homogenates: (B) IL-1β, (C) IL-6, and (D) TNF-α (n=6 mice per group). All quantitative data are presented as mean ± SD. **P < 0.01 versus Control group; ##P < 0.01 versus Model group.

China) at 37°C for 60 minutes. After washing, sections were fixed with 3% H2O2 in methanol for 10 minutes at 25°C to block endogenous peroxidase activity. Subsequently, sections were incubated with converter-peroxidase solution for 35 minutes at 37°C. The sections were then stained with diaminobenzidine (DAB), counterstained with hematoxylin, dehydrated through a graded EtOH series, cleared in xylene, and mounted with resin. The proportion of TUNEL-positive cells was examined under an optical microscope (Leica Camera, Germany).

Enzyme-linked immunosorbent assay (ELISA)

The levels of pro-inflammatory cytokines (TNF-α, IL-1β, and IL-6) in BV-2 cell culture supernatants and mouse hippocampal tissue homogenates were quantified using ELISA kits (eBioscience, USA) according to the manufacturer's instructions, as previously described[22].

Immunohistochemistry

Dewaxed hippocampal sections were subjected to antigen retrieval using a solution from Boster (Wuhan, China). Subsequently, sections were blocked with 5% goat serum and incubated with anti-Iba1 antibody overnight at 4°C. After washing, sections were incubated with the corresponding secondary antibody for 120 minutes at 25°C. Next, sections were stained with diaminobenzidine (DAB), and nuclei were counterstained with hematoxylin (Macklin, China). Finally, the stained sections were visualized and imaged using a BX53 optical microscope.

Cell culture and treatment

The BV-2 microglial cell line was obtained from Procell (Wuhan, China). Cells were cultured in DMEM supplemented with 10% fetal bovine serum (FBS) and 100 μg/mL penicillin-streptomycin at 37°C in a humidified atmosphere containing 5% CO2. BV-2 cells in the logarithmic growth phase were seeded into 96-well plates and incubated overnight. The selection of 200 mM ethanol (EtOH) concentration was based on established protocols from previous studies investigating alcohol-induced microglial activation[23]. This concentration (200 mM) is commonly used for in vitro alcohol exposure experiments to induce reproducible neuroinflammatory responses within 24 hours. While blood alcohol concentrations (BAC) in human chronic alcohol users typically range from 50-100 mM, local ethanol concentrations within the central nervous system (CNS) may reach higher levels (up to 150-200 mM) during binge drinking episodes due to the blood-brain barrier and direct diffusion from the bloodstream. Lower ethanol concentrations (≤100 mM) require prolonged exposure (48-72 hours) to achieve similar effects, which may introduce adaptive tolerance mechanisms that confound result interpretation. Therefore, 200 mM EtOH for 24 hours represents a supraphysiological yet standardized and widely accepted in vitro model for studying acute-on-chronic alcohol-induced neuroinflammation.

Cell transfection

BV-2 cells were seeded into 6-well plates and cultured until they reached 80% confluence. Subsequently, miR-146a-5p mimics, negative control (NC) mimics, pcDNA3.1-Btg2 overexpression vector, and pcDNA3.1 empty vector (all purchased from GenePharm, Shanghai, China) were transfected into the cells using Lipofectamine 3000 (Thermo Fisher Scientific, USA) according to the manufacturer's

protocol. After 24 hours of transfection, cells were collected for further experiments.

Cell counting kit-8 (CCK-8)

BV-2 cells were seeded into 96-well plates at a density of 5,000 cells per well and incubated overnight at 37°C. Then, 10 μL of CCK-8 reagent (Sigma, USA) was added to each well, and the plates were incubated for an additional 2 hours at 37°C. Absorbance was measured at 450 nm using a microplate reader.

Flow cytometry

Briefly, cells were resuspended in 400 μL of pre-cooled PBS and stained with 10 μL of Annexin V-FITC and 5 μL of propidium iodide (PI) (both from BD Biosciences, USA) for 30 minutes at 4°C in the dark. Apoptosis was immediately analyzed by flow cytometry.

RT-qPCR

Total RNA was extracted using TRIzol reagent (Thermo Fisher Scientific, USA). cDNA was synthesized using a High-Capacity cDNA Reverse Transcription Kit (Thermo Fisher Scientific, USA). Quantitative real-time PCR (RT-qPCR) was performed using SYBR Premix Ex Taq II (TaKaRa, Japan) on an ABI 7900HT Real-Time PCR System (Applied Biosystems, USA). Relative gene expression was calculated using the 2-ΔΔCt method. mRNA expression levels were normalized to GAPDH, and miRNA expression levels were normalized to U6 small nuclear RNA. The primer sequences used are listed in Table 1.

Western blot

Total protein concentration was determined using a BCA protein assay kit (Thermo Fisher Scientific, USA). Equal amounts of protein were separated by 10% SDS-PAGE and transferred onto PVDF membranes (Membrane Solutions, Shanghai, China). Membranes were blocked with 5% skim milk for 1 hour at 25°C and then incubated overnight at 4°C with primary antibodies against Bax (1:1000, Abcam, UK), Bcl-2 (1:2000, Abcam, UK), Btg2 (1:200, Abcam, UK), and GAPDH (1:1000, Abcam, UK). After washing, membranes were incubated with horseradish peroxidase (HRP)-conjugated secondary antibodies for 60 minutes at 25°C. Protein bands were visualized using enhanced chemiluminescence (ECL) reagent (Bio-Rad, USA).

Immunofluorescence

BV-2 cells were fixed with 4% paraformaldehyde (PFA) for 20 minutes and permeabilized with 0.5% Triton X-100 for 60 minutes at 25°C. The cells were then incubated overnight at 4°C with a primary antibody against Iba-1 (diluted 1:500, WAKO, Japan). After washing, cells were incubated with fluorescently labeled secondary antibodies (diluted 1:500, Vector Laboratories, USA) for 60 minutes at 25°C in the dark. Nuclei were counterstained with 100 nM DAPI for 15 minutes. Fluorescent images were captured using a fluorescence microscope (Olympus Corporation).

Luciferase reporter assay

Reporter plasmids containing the wild-type (WT) or mutant (MUT) Btg2 3'UTR were synthesized by GenePharma (Shanghai, China). BV-2 cells were cultured until they reached 70% confluence. The Btg2 3'UTR-WT or Btg2 3'UTR-MUT reporter plasmids were co-transfected into BV-2 cells with either miR-146a-5p mimics or NC mimics using Lipofectamine 3000 (Thermo Fisher Scientific, USA). After 48 hours of transfection, luciferase activity was measured using the Dual-Luciferase Reporter Assay System (Promega, USA) according to the manufacturer's protocol.

RNA pull-down assay

The RNA pull-down assay was performed as previously described (24). Briefly, biotin-labeled miR-146a-5p (Bio-miR-146a-5p) and negative control (Bio-NC) probes were synthesized by GenePharm (Shanghai, China). The probes were incubated with Streptavidin-coated Dynabeads M-280 (Invitrogen, USA) at 4°C to form probe-bead complexes. The beads coated with the respective probes were then incubated with cell lysates. After washing, bound RNA was eluted, purified, and analyzed by RT-qPCR.

Statistical analysis

All experiments were performed at least three times independently. Data are presented as mean ± standard deviation (SD). Statistical analyses were performed using GraphPad Prism 10.0 software. Comparisons between two groups were analyzed using Student's t-test. Comparisons among multiple groups were analyzed using one-way analysis of variance (ANOVA) followed by Tukey's post hoc test. A P-value < 0.05 was considered statistically significant.

Results

Overexpressed miR-146a-5p attenuated neuronal apoptosis, inflammation along with microglial activation in EtOH-stimulated BV-2 cells

Recent studies have manifested miR-146a-5p is implicated in nerve damage across various contexts[18]. However, the specific role along with underlying mechanism of miR-146a-5p within alcohol-stimulated nerve damage remain unclear. To investigate this, we first established an in vitro model of chronic alcohol exposure in BV-2 cells by treating them with EtOH. We then measured miR-146a-5p expression through RT-qPCR. Our outcomes revealed that EtOH exposure significantly downregulated miR-146a-5p expression in BV-2 cells. However, miR-146a-5p mimics transfection caused a significant elevation in its expression (Figure 1A). Next, we used the CCK-8 assay for assessing cell viability. EtOH stimulation significantly reduced the viability of BV-2 cells, an effect that was reversed following miR-146a-5p mimics transfection (Figure 1B). Flow cytometry analysis uncovered that EtOH treatment boosted the apoptosis rate of BV-2 cells, but this situation was abolished following miR-146a-5p elevation (Figure 1C). Furthermore, EtOH treatment markedly elevated Bax expression along with diminished Bcl-2 expression in BV-2 cells. However, miR-146a-5p elevation counteracted these changes in EtOH-treated cells (Figure 1D). Long-term alcohol consumption is known to promote the secretion of pro-inflammatory factors along with activate microglia in the brain (25). Therefore, miR-146a-5p's impacts on levels of pro-inflammatory cytokines along with microglial activation in EtOH-treated BV-2 cells were further assessed. As manifested in Figure 1E, EtOH treatment significantly augmented the expression of the microglia marker Iba1, an effect that was weakened following miR-146a-5p overexpression. Similarly, EtOH stimulation notably elevated the levels of pro-inflammatory factors (IL-1β, IL-6, and TNF-α) in BV-2 cells, an effect that was also weakened following miR-146a-5p upregulation (Figure 1F-1H).

MiR-146a-5p targeted Btg2 in BV-2 cells

Then, the molecular target of miR-146a-5p in BV-2 cells was explored. We used starBase website (https://rnasysu.com/encori/index.php) for predicting the possible mRNAs of miR-146a-5p. We selected the top 10 mRNA targets of miR-146a-5p and presented them in Figure 2A. To identify which specific mRNA binds to miR-146a-5p in BV-2 cells, an RNA pull-down assay was conducted. The outcomes showed that, in contrast to the Bio-NC group, Btg2 was significantly enriched in the Bio-miR-146a-5p group. Therefore, Btg2 was chosen for further experimentation (Figure 2B). The binding sequences between the 3'UTR of Btg2 and miR-146a-5p are illustrated in Figure 2C. To confirm whether Btg2 is indeed a target of miR-146a-5p, we employed the luciferase reporter assay. Our findings revealed, in BV-2 cells, transfection with miR-146a-5p mimics diminished the luciferase intensity of the wild-type Btg2 3'UTR, rather than the mutant version, relative to the NC mimics group (Figure 2D). Next, we tested whether miR-146a-5p negatively modulates Btg2 expression in the presence of EtOH treatment. Our results demonstrated that EtOH consistently induces Btg2 expression in BV-2 cells, and such promotion is markedly suppressed following miR-146a-5p amplification (Figure 2E-2F).

MiR-146a-5p attenuated neuronal apoptosis, inflammation along with microglial activation in EtOH-stimulated BV-2 cells via targeting Btg2

To assess if miR-146a-5p can mitigate neuronal apoptosis, inflammation along with microglial activation in BV-2 cells treated with EtOH by targeting Btg2, we first enhanced Btg2 expression in these EtOH-treated cells (Figure 3A-3B). Subsequently, we co-transfected the cells with pcDNA3.1-Btg2 and miR-146a-5p mimics. When treated with EtOH, the elevated cell viability seen in cells transfected with miR-146a-5p mimics was negated upon pcDNA3.1-Btg2 co-transfection (see Figure 3C). Furthermore, the reduction in apoptosis mediated by miR-146a-5p upregulation in EtOH-treated BV-2 cells was abolished following the elevation of Btg2 (Figure 3D). Simultaneously, in the context of EtOH treatment, the depletion in Bax protein level along with the elevation in Bcl-2 protein level, which were initially seen in cells with silenced miR-146a-5p, were abrogated following Btg2 elevation (Figure 3E). Moreover, the introduction of miR-146a-5p mimics cut down the EtOH-stimulated Iba1 expression along with the levels of pro-inflammatory factors (IL-1β, IL-6, and TNF-α) in BV-2 cells. However, this effect was completely abolished by the restoration of Btg2 expression (Figure 3F-3I).

Overexpressed miR-146a-5p exerted a protective effect on alcohol-induced nerve damage in vivo

To assess miR-146a-5p's impact on alcohol-stimulated nerve damage in vivo, a mouse model of chronic alcohol exposure was constructed and miR-146a-5p agomir was subsequently administered to the mice. The findings manifested that miR-146a-5p expression in the hippocampus was diminished in the model mice but was elevated following miR-146a-5p agomir injection (Figure 4A). During a 5-day orientation navigation experiment, the escape latent period in all groups declined, indicating they possessed some level of spatial learning ability. However, the escape latent period in the model group was longer upon comparing to the control group, whereas the escape latent period in the model+miR-146a-5p agomir group was notably shorter upon comparing to the model group (Figure 4B). These results suggest that chronic alcohol consumption negatively affects the learning capacity of mice and that miR-146a-5p agomir administration can enhance mice's learning ability in the model group. On the 6th day, 24 hours after the final training session, we conducted a space exploration experiment. In contrast to the control group, mice with chronic alcohol consumption spent less time in the target quadrant and crossed it fewer times. Nevertheless, compared to the model group, mice in the model+miR-146a-5p agomir group exhibited a significant increase in both the time spent in the target quadrant as well as the frequency of crossings (Figure 4C-4D). These outcomes indicate that chronic alcohol stimulation impairs the spatial memory of mice and that miR-146a-5p agomir administration can mitigate this impairment. Next, through H&E staining, we observed that the hippocampus of model mice exhibited disorganized neuronal layers, severe neuronal damage, pyknosis, and reduced cytoplasm. Following miR-146a-5p overexpression, the hippocampal region displayed clear neuronal layers as well as an elevated number of normal neurons with round nuclei (Figure 4E). Additionally, TUNEL staining demonstrated that the quantity of TUNEL-positive cells in the model group was boosted upon comparing to the control group, whereas miR-146a-5p overexpression caused a reduction in TUNEL-positive cells (Figure 4F). Consistent with these findings, western blot analysis unveiled that in contrast to the control group, Bax protein level was elevated while Bcl-2 protein level was declined in the model group, but this phenomenon was reversed following miR-146a-5p elevation (Figure 4G).

Overexpressed miR-146a-5p exerted a protective impact on alcohol-stimulated neuroinflammation along with microglial activation in vivo

MiR-146a-5p's impacts on alcohol-stimulated neuroinflammation and microglial activation in vivo was evaluated. Immunohistochemical staining indicated an increase in Iba1 protein expression in the model group upon comparing to the control. Nevertheless, miR-146a-5p agomir administration caused a decrease in Iba1 protein expression in the model mice (Figure 5A). Similarly, while pro-inflammatory factors (IL-1β, IL-6, and TNF-α) levels were elevated in the model mice upon comparing to the controls, this elevation was diminished after miR-146a-5p upregulation (Figure 5B-5D).

Discussion

Alcohol is considered as a powerful neurotoxin, which can impact the function of central nervous system, and may also cause neuronal damage by inducing neuronal cell death and neuroinflammation, thus causing neurodegeneration[26]. Regarding alcohol-induced neuronal damage, both drug therapy and non-drug therapy are commonly used intervention methods for patients with alcohol-induced nerve injury. Although they can improve patients' symptoms, the long-term prognosis is poor, and the incidence of adverse reactions during treatment is high, which affects patients' treatment tolerance and compliance[27]. Therefore, actively exploring the mechanism of alcohol-induced nerve injury can provide a reference for clinical intervention.

All cell types in the nervous system are vulnerable to alcohol, which can lead to neuroinflammation[28]. Microglia, serving to be the pivotal immune cells within the central nervous

system, are intimately linked to neuroinflammation[29]. These cells, which belong to the mononuclear phagocytic cell family, are ubiquitously distributed throughout the central system and constitute the smallest subset of glial cells, representing about 5-10% of the total glial population[30]. As resident immune effector cells in the central nervous system, microglia and neuroinflammation they mediate have a crucial role in the damage to the central nervous system[31]. Additionally, microglia are implicated in numerous neurological disorders, including alcohol-induced nerve injury[32]. Under pathological conditions, microglia can become activated, and extensive research has delved into their role in alcohol-related nerve damage[33]. In our study, we observed the activation of microglia in a chronic alcohol exposure model, along with the levels of pro-inflammatory factors containing IL-1β, IL-6, as well as TNF-α, aligning with previous findings[34].

MiR-146a-5p, an inflammation-associated miRNA, has a key role in modulating the pathological process of neurological diseases[35]. For example, it serves as a key affector of neurogenesis in pathological conditions induced by depression[36]. Furthermore, exosomes modified with miR-146a-5p enhances neurological function recovery of rats with acute spinal cord injury[37]. Besides, miR-146a-5p's participation in microglial activation has been well-documented. It accelerates the polarization transitions of microglia linked to advanced glycation end products[38]. Moreover, miR-146a-5p secreted from exosomes of human umbilical cord mesenchymal stem cells significantly reduces microglia activation and the microglial-mediated neuroinflammatory response[39]. In line with these observations, our research revealed that overexpressed miR-146a-5p alleviated neuronal injury, inflammation, and microglial activation in chronic alcohol exposure models.

Furthermore, we discovered that miR-146a-5p bound to its target gene Btg2, and altered Btg2 expression in EtOH-stimulated BV-2 cells. Btg2 is an inflammation-related mRNA and has been reported to enhance inflammatory response in many diseases[40]. For example, Overexpressed Btg2c accelerates inflammation and myocardial injury in myocardial infarction[41]. Btg2 overexpression can induce pro-inflammatory microglial activation in T-2 toxin-induced neurotoxicity[42]. Consistently, our study showed that Btg2 was upregulated in EtOH-treated BV-2 cells. More importantly, Btg2 upregulation was found to counteract the suppressing impacts of elevated miR-146a-5p on neuronal apoptosis, inflammation along with microglial activation in EtOH-treated BV-2 cells. This implies that Btg2 is required for modulating the impacts of miR-146a-5p on these processes in alcohol-induced nerve injury.

Our findings highlight the miR-146a-5p/Btg2 regulatory axis as a promising therapeutic target for alcohol-related neurodegeneration. The specific downregulation of miR-146a-5p following alcohol exposure suggests that its restoration could be a viable strategy. This could be achieved through the development of miR-146a-5p mimics or agomirs designed for targeted CNS delivery. For example, encapsulating miRNA mimics using nanoparticles (such as lipid nanoparticles or polymeric nanoparticles), or utilizing engineered viral vectors (such as adeno-associated virus, AAV) for gene delivery, are common strategies currently employed in research to achieve targeted delivery to the central nervous system. These methods effectively overcome the blood-brain barrier and enhance delivery efficiency. Alternatively, pharmacological or genetic approaches to inhibit Btg2 expression or function might also mitigate neuroinflammatory damage. Future studies should focus on optimizing delivery systems to cross the blood-brain barrier, evaluating the long-term efficacy and safety of such interventions, and exploring potential synergies with existing treatments for alcohol use disorder. Translating these mechanistic insights into clinical applications could open new avenues for preventing or slowing the progression of alcohol-induced cognitive impairment and neural damage.

While our findings provide compelling evidence for the miR-146a-5p/Btg2 axis in alcohol-induced neuroinflammation, several important limitations of this study should be critically acknowledged. First, although we demonstrated specific targeting of Btg2 by miR-146a-5p, the potential off-target effects of miR-146a-5p mimics cannot be completely excluded. miRNAs are known to regulate multiple mRNA targets, and some of the observed protective effects might be partially mediated through other pathways, such as TRAF6 or IRAK1, which are also established targets of miR-146a-5p. Second, and most importantly, all our in vitro experiments were conducted exclusively in the BV-2 murine microglial cell line. While BV-2 cells are a widely accepted and convenient model for initial mechanistic studies, they are an immortalized cell line that differs from primary microglia in several critical aspects. Compared to primary microglia, BV-2 cells exhibit altered expression profiles of inflammation-related genes, attenuated phagocytic capacity, and exaggerated cytokine responses to certain stimuli. These differences may influence the magnitude and even the direction of observed effects, potentially limiting the direct translational relevance of findings derived solely from this cell line. Third, we did not validate our key findings in primary microglial cultures (either murine or human) or in human post-mortem brain tissue from individuals with alcohol use disorder. The lack of human sample validation represents a significant gap, as cross-species differences in miRNA expression patterns, target specificity, and immune responses are well documented. Fourth, our in vivo experiments were conducted only in male C57BL/6 mice, leaving the potential sex-dependent effects of the miR-146a-5p/Btg2 axis unexplored. Given the known sex differences in both alcohol metabolism and neuroinflammatory responses, this is a notable omission that should be addressed in future studies. Future studies utilizing primary mouse microglia, human induced pluripotent stem cell (iPSC)-derived microglia, and post-mortem brain tissues from alcohol use disorder patients will be essential to validate and extend our observations. Additionally, the development of conditional microglia-specific Btg2 knockout mice would provide more definitive genetic evidence for the in vivo function of this pathway. We acknowledge these limitations as important caveats and emphasize that our findings should be interpreted as hypothesis-generating rather than definitive.

The identification of the miR-146a-5p/Btg2 axis as a critical regulator of alcohol-induced neuroinflammation opens up several avenues for clinical translation. First, miRNA-based therapeutics have emerged as a promising class of drugs, with several miRNA mimics and antagomirs currently in clinical trials for various diseases (e.g., MRG-106 for cutaneous T-cell lymphoma, MRX34 for hepatocellular carcinoma). Our finding that miR-146a-5p is downregulated following chronic alcohol exposure suggests that restoring its expression using synthetic miRNA mimics or agomirs could represent a viable therapeutic strategy. Second, effective CNS delivery remains

https://dx.doi.org/10.4314/mmj.v38i2.12

a key challenge for miRNA therapeutics. Recent advances in nanotechnology have enabled the development of blood-brain barrier (BBB)-crossing delivery systems, including lipid nanoparticles (LNPs) functionalized with targeting ligands (e.g., rabies virus glycoprotein-derived peptides, transferrin receptor antibodies), exosome-based carriers, and engineered adeno-associated virus (AAV) vectors with microglial tropism. These platforms could be leveraged to deliver miR-146a-5p mimics specifically to microglia, potentially minimizing systemic side effects. Third, beyond direct miRNA replacement, Btg2 itself may represent a druggable target. While small-molecule inhibitors of BTG2 have not yet been developed, the structural characterization of the BTG2 protein could facilitate virtual screening and rational drug design. Alternatively, existing compounds that modulate pathways upstream of BTG2 (e.g., PI3K/AKT/FOXO3a signaling) could be repurposed. Fourth, the expression level of miR-146a-5p in peripheral blood or cerebrospinal fluid could serve as a predictive biomarker for alcohol-induced neuroinflammation and cognitive impairment. Patients with persistently low miR-146a-5p levels despite abstinence might be prioritized for anti-neuroinflammatory interventions. Fifth, combining miR-146a-5p restoration with existing treatments for alcohol use disorder, such as naltrexone, acamprosate, or psychosocial interventions, could produce synergistic effects by simultaneously addressing craving/relapse prevention (via conventional pharmacotherapy) and neuroinflammation/neuroprotection (via miRNA therapy). Future research should prioritize large-animal safety and efficacy studies, optimization of BBB-penetrant delivery systems, and carefully designed Phase I/II clinical trials in well-characterized patient populations. While significant hurdles remain, the miR-146a-5p/Btg2 axis represents a mechanistically grounded and therapeutically tractable target for mitigating alcohol-induced neurodegeneration.

In summary, our paper provides compelling evidence that miR-146a-5p mitigates alcohol-induced neuroinflammation and microglial activation by directly targeting Btg2. These findings not only elucidate a novel molecular pathway but also strongly suggest that the miR-146a-5p/Btg2 axis holds significant promise as a potential therapeutic target for alcohol-induced nerve injury.

Declarations

Ethics approval and consent to participate

All animal experiments were reviewed and approved by the Experimental Animal Care and Use Committee of The Fifth People's Hospital of Kaifeng, China, and conducted in accordance with the National Institutes of Health Guide for the Care and Use of Laboratory Animals. This study did not involve any human participants; therefore, informed consent was not required.

Consent for publication

Not applicable.

Availability of data and materials

The datasets used and/or analyzed during the current study are available from the corresponding author upon reasonable request.

Competing interests

The authors declare that they have no competing interests.

Funding

This research received no specific grant from any funding agency in the public, commercial, or not-for-profit sectors.

Authors' contributions

Bo Cheng designed and supervised the study. Yan Wang and Ping Huang performed the experiments and analyzed the data. Zikuo Dong and Junya Zhou contributed to statistical analysis. Guoqing Kang, Chengzhu Wang, and Zhenkun Yan assisted in data interpretation and manuscript editing. All authors read and approved the final manuscript.

Acknowledgements

The authors thank the Department of Substance Dependence and the Department of Psychiatry I of The Fifth People's Hospital of Kaifeng for their assistance and technical support.

References

1.Im PK, Wright N, Yang L, Chan KH, Chen Y, Guo Y, et al. Alcohol consumption and risks of more than 200 diseases in Chinese men. Nat Med. 2023;29(6):1476-86.

2.Mirijello A, Sestito L, Antonelli M, Gasbarrini A, Addolorato G. Identification and management of acute alcohol intoxication. Eur J Intern Med. 2023;108:1-8.

3.Lam HYP, Liang TR, Peng SY. Prevention of the Pro-Aggressive Effects of Ethanol-Intoxicated Mice by Schisandrin B. Nutrients. 2023;15(8).

4.Togre NS, Mekala N, Bhoj PS, Mogadala N, Winfield M, Trivedi J, et al. Neuroinflammatory responses and blood-brain barrier injury in chronic alcohol exposure: role of purinergic P2 × 7 Receptor signaling. J Neuroinflammation. 2024;21(1):244.

5.Fujii C, Zorumski CF, Izumi Y. Ethanol, neurosteroids and cellular stress responses: Impact on central nervous system toxicity, inflammation and autophagy. Neurosci Biobehav Rev. 2021;124:168-78.

6.Egervari G, Siciliano CA, Whiteley EL, Ron D. Alcohol and the brain: from genes to circuits. Trends Neurosci. 2021;44(12):1004-15.

7.Banerjee S, Park T, Kim YS, Kim HY. Exacerbating effects of single-dose acute ethanol exposure on neuroinflammation and amelioration by GPR110 (ADGRF1) activation. J Neuroinflammation. 2023;20(1):187.

8.Borst K, Dumas AA, Prinz M. Microglia: Immune and non-immune functions. Immunity. 2021;54(10):2194-208.

9.Long Y, Li XQ, Deng J, Ye QB, Li D, Ma Y, et al. Modulating the polarization phenotype of microglia - A valuable strategy for central nervous system diseases. Ageing Res Rev. 2024;93:102160.

10.Kwon HS, Koh SH. Neuroinflammation in neurodegenerative disorders: the roles of microglia and astrocytes. Transl Neurodegener. 2020;9(1):42.

11.Singh S, Kannan M, Oladapo A, Deshetty UM, Ray S, Buch S, et al. Ethanol modulates astrocyte activation and neuroinflammation via miR-339/NLRP6 inflammasome signaling. Free Radic Biol Med. 2025;226:1-12.

12.Ruiz GP, Camara H, Fazolini NPB, Mori MA. Extracellular miRNAs in redox signaling: Health, disease and potential therapies. Free Radic Biol Med. 2021;173:170-87.

13.Giannubilo SR, Cecati M, Marzioni D, Ciavattini A. Circulating miRNAs and Preeclampsia: From Implantation to Epigenetics. Int J Mol Sci. 2024;25(3).

14.Shang R, Lee S, Senavirathne G, Lai EC. microRNAs in action: biogenesis, function and regulation. Nat Rev Genet. 2023;24(12):816-33.

15.Salim U, Kumar A, Kulshreshtha R, Vivekanandan P. Biogenesis,

characterization, and functions of mirtrons. Wiley Interdiscip Rev RNA. 2022;13(1):e1680.

16.Winkler I, Engler JB, Vieira V, Bauer S, Liu YH, Di Liberto G, et al. MicroRNA-92a-CPEB3 axis protects neurons against inflammatory neurodegeneration. Sci Adv. 2023;9(47):eadi6855.

17.Chen ML, Hong CG, Yue T, Li HM, Duan R, Hu WB, et al. Inhibition of miR-331-3p and miR-9-5p ameliorates Alzheimer's disease by enhancing autophagy. Theranostics. 2021;11(5):2395-409.

18.Zhou H, Yang RK, Li Q, Li Z, Wang YC, Li SY, et al. MicroRNA-146a-5p protects retinal ganglion cells through reducing neuroinflammation in experimental glaucoma. Glia. 2024;72(11):2115-41.

19.Lu Y, Cao DL, Jiang BC, Yang T, Gao YJ. MicroRNA-146a-5p attenuates neuropathic pain via suppressing TRAF6 signaling in the spinal cord. Brain Behav Immun. 2015;49:119-29.

20.Lin X, Li X, Li C, Wang H, Zou L, Pan J, et al. Activation of STING signaling aggravates chronic alcohol exposure-induced cognitive impairment by increasing neuroinflammation and mitochondrial apoptosis. CNS Neurosci Ther. 2024;30(3):e14689.

21.Li D, Yang H, Ma J, Luo S, Chen S, Gu Q. MicroRNA-30e regulates neuroinflammation in MPTP model of Parkinson's disease by targeting Nlrp3. Hum Cell. 2018;31(2):106-15.

22.Guo LT, Wang SQ, Su J, Xu LX, Ji ZY, Zhang RY, et al. Baicalin ameliorates neuroinflammation-induced depressive-like behavior through inhibition of toll-like receptor 4 expression via the PI3K/AKT/FoxO1 pathway. J Neuroinflammation. 2019;16(1):95.

23.Asatryan L, Ostrovskaya O, Lieu D, Davies DL. Ethanol differentially modulates P2X4 and P2X7 receptor activity and function in BV2 microglial cells. Neuropharmacology. 2018;128:11-21.

24.Chen J, Chen T, Zhu Y, Li Y, Zhang Y, Wang Y, et al. circPTN sponges miR-145-5p/miR-330-5p to promote proliferation and stemness in glioma. J Exp Clin Cancer Res. 2019;38(1):398.

25.Pradier B, Erxlebe E, Markert A, Rácz I. Microglial IL-1β progressively increases with duration of alcohol consumption. Naunyn Schmiedebergs Arch Pharmacol. 2018;391(4):455-61.

26.Wood EK, Lemmon DP, Schwandt ML, Lindell SG, Barr CS, Suomi SJ, et al. Central nervous system monoamine metabolite response to alcohol exposure is associated with future alcohol intake in a nonhuman primate model (Macaca mulatta). Addict Biol. 2022;27(3):e13142.

27.Serrano M, Rico-Barrio I, Grandes P. The effect of omega-3 fatty acids on alcohol-induced damage. Front Nutr. 2023;10:1068343.

28.Leng F, Edison P. Neuroinflammation and microglial activation in Alzheimer disease: where do we go from here? Nat Rev Neurol. 2021;17(3):157-72.

29.Peruzzotti-Jametti L, Willis CM, Krzak G, Hamel R, Pirvan L, Ionescu RB, et al. Mitochondrial complex I activity in microglia sustains neuroinflammation. Nature. 2024;628(8006):195-203.

30.Barry-Carroll L, Gomez-Nicola D. The molecular determinants of microglial developmental dynamics. Nat Rev Neurosci. 2024;25(6):414-27.

31.Terzioglu G, Young-Pearse TL. Microglial function, INPP5D/SHIP1 signaling, and NLRP3 inflammasome activation: implications for Alzheimer's disease. Mol Neurodegener. 2023;18(1):89.

32.Alfonso-Loeches S, Pascual-Lucas M, Blanco AM, Sanchez-Vera I, Guerri C. Pivotal role of TLR4 receptors in alcohol-induced neuroinflammation and brain damage. J Neurosci. 2010;30(24):8285-95.

33.Portis SM, Haass-Koffler CL. New Microglial Mechanisms Revealed in Alcohol Use Disorder: How Does That Translate? Biol Psychiatry. 2020;88(12):893-5.

34.Shrivastava P, Cabrera MA, Chastain LG, Boyadjieva NI, Jabbar S, Franklin T, et al. Mu-opioid receptor and delta-opioid receptor differentially regulate microglial inflammatory response to control proopiomelanocortin neuronal apoptosis in the hypothalamus: effects of neonatal alcohol. J Neuroinflammation. 2017;14(1):83.

35.Jia L, Zhu M, Yang J, Pang Y, Wang Q, Li Y, et al. Prediction of P-tau/Aβ42 in the cerebrospinal fluid with blood microRNAs in Alzheimer's disease. BMC Med. 2021;19(1):264.

36.Fan C, Li Y, Lan T, Wang W, Long Y, Yu SY. Microglia secrete miR-146a-5p-containing exosomes to regulate neurogenesis in depression. Mol Ther. 2022;30(3):1300-14.

37.Lai X, Wang Y, Wang X, Liu B, Rong L. miR-146a-5p-modified hUCMSC-derived exosomes facilitate spinal cord function recovery by targeting neurotoxic astrocytes. Stem Cell Res Ther. 2022;13(1):487.

38.Huang Y, Lin X, Lin X. MiR-146a-5p Contributes to Microglial Polarization Transitions Associated With AGEs. Mol Neurobiol. 2023;60(6):3020-33.

39.Zhang Z, Zou X, Zhang R, Xie Y, Feng Z, Li F, et al. Human umbilical cord mesenchymal stem cell-derived exosomal miR-146a-5p reduces microglial-mediated neuroinflammation via suppression of the IRAK1/TRAF6 signaling pathway after ischemic stroke. Aging (Albany NY). 2021;13(2):3060-79.

40.Kong L, Liu Y, Wang JH, Lv MJ, Wang YZ, Sun WP, et al. Linggui Zhugan decoction ameliorating mitochondrial damage of doxorubicin-induced cardiotoxicity by modulating the AMPK-FOXO3a pathway targeting BTG2. Phytomedicine. 2025;139:156529.

41.Ruan Y, Meng S, Jia R, Cao X, Jin Z. MicroRNA-322-5p protects against myocardial infarction through targeting BTG2. Am J Med Sci. 2024;367(6):397-405.

42.Li X, Long J, Yao C, Liu X, Li N, Zhou Y, et al. The role of BTG2/PI3K/AKT pathway-mediated microglial activation in T-2 toxin-induced neurotoxicity. Toxicol Lett. 2024;400:81-92.